N-Homocysteinylation Impairs Collagen Crosslinking In Cystathionine β-Synthase-Deficient Mice: A Novel Mechanism of Connective Tissue Abnormalities*

Joanna Perła-Kajan[†], Olga Utyro[‡], Marta Rusek[¶, 2], Agata Malinowska[$], Ewa Sitkiewicz[$], and Hieronim Jakubowski [†, ‡, ¶,1]

From the [†]Department of Biochemistry and Biotechnology, University of Life Sciences, Poznań; [‡]Institute of Bioorganic Chemistry, Poznań, Poland; [$]Proteomics Laboratory, Biophysics Department, Institute of Biochemistry and Biophysics, Warsaw; [¶]Department of Microbiology, Biochemistry and Molecular Genetics, Rutgers University, New Jersey Medical School, International Center for Public Health, Newark, NJ 07103, USA

[1] Correspondence: Prof. Hieronim Jakubowski, Department of Microbiology, Biochemistry and Molecular Genetics, Rutgers-New Jersey Medical School, International Center for Public Health, 225 Warren Street, Newark, New Jersey 07103, USA, Tel: 973-972-8733; Fax: 973-972-8981; E-mail: jakubows@rutgers.edu

[2] Permanent affiliation: Department of Pathophysiology, Medical University, Lublin, Poland

Running Title: Collagen *N*-homocysteinylation impairs crosslinking

ABSTRACT Cystathionine β-synthase (CBS) deficiency, a genetic disorder in homocysteine (Hcy) metabolism in humans, elevates plasma Hcy-thiolactone and leads to connective tissue abnormalities affecting cardiovascular and skeletal systems. However, the underlying mechanism of these abnormalities is not understood. Hcy-thiolactone has the ability to form isopeptide bonds with protein lysine residues, which generates *N*-homocysteinylated protein. Because lysine residues are involved in collagen crosslinking, *N*-homocysteinylation of these lysines should impair crosslinking. Using a *Tg-I278T Cbs*$^{-/-}$ mouse model of hyperhomocysteinamia (HHcy) that recapitulates connective tissue abnormalities observed in CBS-deficient patients, we show that *N*-Hcy-collagen was elevated in bone, tail, and heart of *Cbs*$^{-/-}$ mice, while pyridinoline crosslinks were significantly reduced. Plasma deoxypyridinoline crosslink and crosslinked carboxyterminal telopeptide of type I collagen were also significantly reduced in *Cbs*$^{-/-}$ mice. Lysine oxidase activity and mRNA level were not reduced by the *Cbs*$^{-/-}$ genotype. We also show that collagen carries *S*-linked Hcy bound to the thiol of *N*-linked Hcy. *In vitro* experiments show that Hcy-thiolactone modifies lysine residues in collagen type I alpha-1 chain. Residue K160, located in the non-helical *N*-telopeptide region and involved in pyridinoline crosslink formation, was also *N*-homocysteinylated *in vivo*. Taken together, our findings show that *N*-homocysteinylation of collagen in *Cbs*$^{-/-}$ mice impairs its crosslinking. These findings explain at least in part connective tissue abnormalities observed in HHcy.

Key Words: *hyperhomocysteinemia, homocysteine thiolactone, collagen modification, pyridinoline crosslinks, N-telopeptide, Col1A1*

Homocysteine (Hcy) is an intermediary metabolite that arises from the metabolism of the essential dietary protein amino acid methionine (Met). Hcy levels are regulated by remethylation to Met, catalyzed by Met synthase (with methyltetrahydrofolate cofactor provided by the MTHFR enzyme) and betaine-Hcy methyltransferase, as well as by transsulfuration to cysteine, the first step of which is catalyzed by cystathionine β-synthase (CBS) (1).

Hcy is also metabolized to the thioester Hcy-thiolactone in an error-editing reaction in protein biosynthesis when Hcy is erroneously selected in place of Met by methionyl-tRNA synthetase (MetRS) (2). Hcy-thiolactone forms isopeptide bonds with protein lysine residues, generating *N*-Hcy-protein in a process called *N*-homocysteinylation (3-5).

Genetic or nutritional deficiencies in Hcy metabolism lead to hyperhomocysteinemia (HHcy) characterized by the accumulation in the blood and tissues of Hcy, Hcy-thiolactone and *N*-Hcy-protein, which have been linked to neurological and cardiovascular diseases (6). For example, Hcy-thiolactone is a predictor of acute myocardial infarction in patients with angiographically confirmed cardiovascular disease in a large randomized controlled clinical trial with over 2000 patients (7).

In humans, severe HHcy due to *CBS* deficiency causes connective tissue abnormalities in most body systems, including bones and vasculature (1). HHcy due to MTHFR deficiency has also been linked to bone abnormalities in humans (8, 9). Similar connective tissue abnormalities affecting bones are also observed in *Cbs*$^{-/-}$ mice (10, 11).

Collagen is a major component of fibrous connective tissues such as tendons and bone (12). It is the most abundant protein and accounts for 25-35% of total body protein content in mammals. Collagenous fibers provide structural support and resistance to stretch forces. Mechanical properties of collagenous fibers come from specific inter-chain crosslinks involving lysine residues within and between collagen chains (13). The crosslink formation is initiated by the conversion of specific lysine and hydroxylysine resides to the aldehydes allysine and hydroxyallysine, respectively, catalyzed by lysine oxidase (LOX) (14, 15). The allysine or hydroxyallysine and ε-amino group of a neighboring lysine residue react spontaneously to form a Schiff-base adduct, which matures into a stable pyridinoline crosslink (16). There are one to two crosslinks per triple helical collagen unit. The main fibril-forming collagens (type I, II, and III) have four cross-linking sites, one in each of the short non-helical ends of collagen molecules (telopeptides) and two in the triple helical region, close to its *N*- and *C*-terminal ends. The pyridinoline crosslinks occur in bone, skeletal tissues, and cartilage collagens and provide the tensile strength and mechanical stability of collagen fibrils, required for normal function of connective tissues (12, 13).

Mechanisms by which HHcy causes connective tissue abnormalities are not understood. Because collagen lysine residues are involved in crosslink formation, *N*-homocysteinylation of these lysines should impair crosslinking (3, 17). To examine this prediction, we studied collagen *N*-homocysteinylation and crosslinking in tissues of *Cbs*$^{-/-}$ mice and their *Cbs*$^{+/-}$ littermates.

MATERIALS AND METHODS

Mice

Transgenic *Tg-I278T Cbs*$^{-/-}$ mice on C57BL/6J genetic background (11) and their *Cbs*$^{+/-}$ littermates were bred and housed at the Rutgers-New Jersey Medical School Animal Facility. In these animals, the human *CBS-I278T* variant is under control of the zinc-inducible metallothionein promoter, which allows rescue the neonatal lethality phenotype of *Cbs*$^{-/-}$ in mice by supplementing the drinking water of pregnant dams with 25 mM zinc chloride. Zinc water is replaced by plain water after weaning.

Tg-I278T Cbs$^{-/-}$ mice exhibit facial alopecia, osteoporosis (rough periosteal surface and small holes in femur, reduced trabecular bone mass, decreased bone mineral density), endoplasmic reticulum stress in the liver and kidney, and life span reduced by 20% (11). *Tg-I278T Cbs*$^{-/-}$ mice also exhibit a thin, smooth, and shiny tail and have significantly lower body weight than their *Cbs*$^{+/-}$ littermates (males: 23.8.3±2.2 *vs*. 27.9±1.9 g, n=14 each group, *P*=0.0001; females 18.8±1.2 vs. 24.3±1.9 g, n=5 each group, *P*=0.004). The mice were fed a normal rodent chow (LabDiet5010, Purina Mills International, St. Louis, MO). Six to nine month-old mice of both sexes were used in experiments. Animal procedures were approved by the Institutional Animal Care and Use Committee at the Rutgers-New Jersey Medical School.

tHcy, *S*-Hcy, and *N*-Hcy assays

tHcy, *S*-Hcy, and *N*-Hcy were assayed by the conversion to Hcy-thiolactone, which was then separated by cation exchange HPLC, post-column derivatized with OPA, detected and quantified by fluorescence as previously described (18). Agilent Infinity 1260 system, containing HiP degasser, binary pump, high performance auto-sampler, thermostated column compartment, diode array detector, and fluorescence detector was used. Samples (5 µL) were injected into Poly CAT A column, 35x2.1 mm, 5 µM, 300 Å (Poly LC).

Plasma and urinary tHcy assays

Mouse plasma or urine (10 µL) was diluted to 100 µL with 20 mM K_2HPO_4, 2 mM dithiothreitol (DTT), and ultra-filtered on Amicon 10 kD cut off devices (4°C, 14,000 g, 30 min). Hcy in the filtrate (30 µL) was converted to Hcy-thiolactone by the treatment with 2 µL 0.25 M DTT, 5 µL 6 N HCl (100°C 30 min). D,L-Hcy standards (1.25-10 µM in 20 mM K_2HPO_4) were treated in the same manner. Tested

samples and standards were dried, dissolved in water (30 µL) and Hcy-thiolactone was quantified by cation exchange HPLC.

Urinary Hcy-thiolactone and *N*-Hcy-protein assays

Urine (10 µL) was neutralized with K_2HPO_4. Hcy-thiolactone was extracted from the neutralized urine using the chloroform/methanol method (19, 20) and quantified by HPLC (21). To quantify *N*-Hcy-protein, the neutralized urine (10 µL) was diluted 50-fold, treated with 2 mM DTT, and free Hcy removed by ultrafiltration using 3 kDa molecular weight cut-off Sartorius centrifugal ultrafiltration devices. The dilution-ultrafiltration cycle was repeated 5 more times to assure complete removal of free Hcy, confirmed by quantifying Hcy in protein-free filtrates. *N*-Hcy-protein was hydrolyzed under reducing conditions, under which liberated *N*-linked Hcy is quantitatively converted to Hcy-thiolactone, which was then extracted with chloroform/methanol, and quantified by cation exchange HPLC (22).

Tissue tHcy and *N*-Hcy-protein assays

Frozen mouse tissue (about 50 mg) was transferred to 10 volumes of ice-cold 20 mM potassium phosphate buffer (pH 7.4), 0.2 mM EDTA containing protease inhibitor mixture (Sigma-Aldrich) and disintegrated by sonication on wet ice. Bone (hind leg tibia and femur) was pulverized with dry ice using a pestle and mortar pre-chilled to -80°C, prior to sonication. Crude extracts were clarified by centrifugation (15,000g, 15 min) and supernatants and pellets were saved. Protein in the supernatant was quantified using a Coomassie protein assay reagent (Sigma-Aldrich) according to the Bradford method (23).

To quantify tissue tHcy, the supernatant (50 µL) was treated with 25 mM DTT, 20 mM K_2HPO_4 (50 µL) and deproteinized by ultrafiltration using Amicon 10 kDa molecular weight cut-off devices. Reduced Hcy in the protein-free filtrate (30 µL) was converted to Hcy-thiolactone by the treatment with DTT (2 µL 0.25 M) and HCl (5 µL 6N, 100°C, 30 min). In parallel, D,L-Hcy standards (1.25-10 µM in 20 mM K_2HPO_4) were treated in the same manner. After the conversion, reaction mixtures were dried under vacuum using a Labconco Centri-Vap concentrator, dissolved in deionized water, and Hcy-thiolactone was quantified by HPLC.

To quantify tissue *N*-Hcy-protein, free Hcy was removed from the protein left on ultrafiltration devices by 4 cycles of dilution with 450 µL 20 mM K_2HPO_4, 2 mM DTT and ultra-filtration. After the last cycle, protein was quantified using the Bradford method, transferred to a glass ampule, and hydrolyzed with 6 N HCl, 20 mM DTT (120°C, 1 h). The hydrolysats were dried and stored at -80°C for Hcy-thiolactone quantification.

S- and N-Hcy determination in bone collagen

Pellets after tissue homogenization and centrifugation were washed with 100 mM potassium phosphate buffer (pH 7.4), 0.2 mM EDTA (4 times, 300 µL). After the last wash, pellets were treated with 20 mM potassium phosphate (pH 7.4), 0.2 mM EDTA, 20 mM DTT (50 µL, 25°C, 5 min) to liberate disulfide-bound Hcy and clarified by centrifugation. Hcy in the resulting supernatant was converted to Hcy-thiolactone, which was then quantified by HPLC. To quantify collagen Hyp, *N*-Hcy, and pyridinolines, the pellet was washed twice with 1 mL of 20 mM K_2HPO_4 containing 2 mM DTT, dried, and transferred to dark glass ampules, containing 15 µL water, 25 µL 20 mM K_2HPO_4, and 40 µL 12 N HCl. The ampoules were frozen on dry ice, sealed under vacuum, and hydrolyzed at 120°C for 1 hr. Hydrolysates were dried, dissolved in 30 µL water and one half (15 µL) was used for *N*-Hcy determination and the other half for Hyp and pyridinoline assays.

_S_- and _N_-Hcy determination in acid-soluble tail collagen

Following tissue homogenization, insoluble pellets were collected by centrifugation, washed with 100 mM potassium phosphate buffer (pH 7.4) containing 0.2 mM EDTA and protease inhibitor (Sigma-Aldrich), defatted with chloroform/methanol mixture (2:1, v/v), and washed again with the buffer. Pellets were extracted with 0.5 M acetic acid containing 0.1 mg/mL pepsin (4°C, 24 h) and the extracts clarified by centrifugation (18,000 g, 15 min). Supernatants containing acid-soluble collagen were dried using a Labconco CentriVap concentrator.

To quantify *S*-Hcy and *N*-Hcy, dried acid-soluble collagen preparations were treated with 20 mM DTT, 20 mM K_2HPO_4 (50 µL, 25°C, 5 min) and clarified by centrifugation (18,000 g, 30 min). *S*-Hcy in the supernatants (30 µL) was converted to Hcy-thiolactone and quantified by HPLC (22, 24).

To quantify *N*-Hcy, collagen pellets were washed twice with 20 mM K_2HPO_4, 2 mM DTT (500 µL) to remove residual free Hcy, dried, and hydrolyzed with 6 N HCl, 30 mM DTT (120°C, 1 h). The hydrolysates were dried, the resulting Hcy-thiolactone was solid-phase extracted (see below), and quantified by cation exchange HPLC (22).

Solid phase extraction of Hcy-thiolactone from protein hydrolysates

Hcy-thiolactone was extracted from tissue protein hydrolysates using reversed phase C18 sorbent in Empore C18-SD, 7 mm/3 mL extraction disk cartridge (Supelco). The C18 sorbent was first conditioned with acetonitrile, water and 10 mM sodium phosphate, pH 7.7 (500 µL each). Dried protein hydrolysates were dissolved in 50 µL of 1M K_2HPO_4, diluted to 1 mL with 10 mM sodium phosphate, pH 7.7, and transferred into the extraction disk cartridge. Because under these conditions Hcy-thiolactone is neutral (pK_a=6.67, (25)), it is retained on a C18 sorbent. After unbound substances were washed off the cartridge with 500 µL of 10 mM sodium phosphate, pH 7.7, Hcy-thiolactone was eluted with 500 µL of 70% acetonitrile containing 0.02 M HCl. At acidic pH Hcy-thiolactone becomes

positively charged and is released from the C18 sorbent (20). Eluents were dried and stored at -80°C for Hcy-thiolactone quantification by cation exchange HPLC (22).

Determination of pyridinoline crosslinks

Collagen pyridinoline crosslinks were quantified by HPLC (26). Collagen was acid-hydrolyzed (6 N HCl, 110°C, 24 h) and pyridinolines were separated on a cation exchange polysulfoethyl aspartamide (PSEA) column, 100x2.1 mm, 3 µM, 300 Å (Poly LC) using a salt gradient at flow rate 0.36 mL/min at 24°C. Solvent A was 0.1% trifluoroacetic acid, solvent B, 1 M NaCl. The gradient was as follows: 15% to 50% B for 8 min, 50% B from 8 to 9 min, and re-equilibration with 15 % B from 9.1 to 11 min. Pyridinoloine (Pyd) and deoxypyridinoline (Dpd) elute as a single peak, detected and quantified by fluorescence with excitation at 295 nm and emission at 395 nm. Authentic Pyd and Dpd (cat. no. 8004, Quidel Corp., San Diego, CA) were used as standards.

Hydroxyproline assay

Hydroxyproline (Hyp) was quantified using the chloramine method (27). Protein hydrolysates (3 µL) diluted with water to 40 µL were incubated with 20 µL of chloramine-T solution (50 mM chloramine-T, 30% (v/v) ethylene glycol monomethylether, 50% chloramine-T buffer, pH 6.0 (0.26 M citric acid, 1.46 M sodium acetate, 0.85 M sodium hydroxide, 1.2% (v/v) glacial acetic acid; 25°C, 20 min). Reaction mixtures were then treated with perchloric acid (3.15 M, 20 µL; 25°C, 5 min) and Ehrlich's solution (1.34 M p-dimethylaminobenzaldehyde ether, 20 µL; 60°C, 20 min). The absorbance was read at 595 nm in ELx808 BioTek plate reader.

Cross-linked C-telopeptide of type I collagen and carboxyterminal propeptide of type I procollagen assays

Cross-linked C-telopeptide of type I collagen (CTXI) and procollagen I C-terminal propeptide (PICP) in mouse plasma were quantified using commercial Enzyme-linked Immunosorbent Assays kits (Cloud-Clone Corp. and Blue Gene, respectively), in which tested CTXI or PICP from samples competes with horse radish peroxidase-labeled CTXI or PICP for binding to a CTXI- or PICP-specific antibody pre-coated onto a microplate. Samples were analyzed in duplicates following manufacturer's protocol.

Analysis of collagen *N*-homocysteinylation by mass spectrometry

Rat tail or mouse bone collagen type I (10 mg/ml) was modified with L-Hcy-thiolactone (10 mM) (Sigma-Aldrich) in 0.1 M phosphate buffer pH 7.4 as previously described (28). Resulting *N*-Hcy-collagen was reduced with 0.1M DTT (56°C, 30 min) or 5 mM tris(2-carboxyethyl) phosphine (TCEP) (room temperature, 1 h), carboxyamidomethylated with 0.5 M iodoacetamide (IAA) (room temperature, 45 min) or methylthiolated with 10 mM methyl metanethiosulfonate (MMTS) (room

temperature, 10 min) to block free thiols, and digested overnight with 10 ng/µL trypsin (Promega). Mouse bone collagen was isolated from *Cbs*$^{-/-}$ and wild type animal using the acetic acid/pepsin extraction method (29) and processed as above to generate tryptic peptides (30). Tryptic peptides were concentrated and desalted on a RP-C18 pre-column (Waters).

Analyses of collagen tryptic peptides were carried by LC-MS/MS. Peptides were separated on a nano-Ultra Performance Liquid Chromatography (UPLC) RP-C18 column (Waters, BEH130 C18 column, 25 cm x 75 µm i.d.) using a nanoACQUITY UPLC system, and a 160-min gradient of 5-30 % acetonitrile at a 300 nl/min flow rate.

The UPLC system was interfaced with micrOTOF-q mass spectrometer electrospray ionization ion source of the Orbitrap Elite type mass spectrometer (Thermo) working in the regime of data dependent MS to MS/MS switch with HCD type peptide fragmentation (30). An electrospray voltage of 2 kV was used. Raw data files were pre-processed with Mascot Distiller software (version 2.4.2.0, MatrixScience). Peptide masses and fragmentation spectra were matched to the National Centre Biotechnology Information (NCBI) non-redundant database (57412064 sequences/20591031683 residues), with a Rodentia filter (733975 sequences) using the Mascot search engine (Mascot Daemon v. 2.4.0, Mascot Server v. 2.4.1, MatrixScience). The search parameters were as follows: enzyme specificity – semi-trypsin; variable modifications – oxidation (M), carbamidomethylation (C), de-methylation (M), and methylatiolation (C). The *N*-Hcy-Lys modification was added to the MASCOT database as *S*-carbamidomethyl- or *S*-methylthio-Hcy. Mass increase due to Lys modification by *S*-carbamidomethyl- or *S*-methylthio-Hcy is 174 Da or 163 Da, respectively. The protein mass was left as unrestricted, and mass values as monoisotopic with one missed cleavage allowed. The peptide and fragment ion mass tolerances were determined separately for individual LC–MS/MS runs by a procedure based on two database searches with an intermittent mass measurement error recalibration step, using an DatViewer software developed in-house (http://proteom.ibb.waw.pl/mscan/) (30). The statistical significance of each peptide identification was estimated using a joined target/decoy database search approach, false discovery rate was set below 1%.

LOX activity assay

We used LOX activity assay kit (Abcam, ab112139) to quantify LOX activity in the heart and liver of *Cbs*$^{-/-}$ and *Cbs*$^{+/-}$ mice. The assay quantifies hydrogen peroxide generated by LOX using a proprietary red fluorescence substrate in a horseradish peroxidase-coupled reaction.

Mouse tissues (heart, 30 mg; liver, 50 mg) were homogenized by sonication with 10 volumes of ice-cold RIPA buffer containing protease inhibitors (Sigma-Aldrich). Cell debris were separated by centrifugation at 15,000 g for 15 min and the resulting supernatants were used for LOX activity

measurement. Protein concentration was measured using the Bradford method. To eliminate any unspecific fluorescence signal, one set of tissue extracts was pre-incubated (37°C, 30 min) with 25 mM D,L-Hcy thiolactone, an irreversible inhibitor of LOX (31), while another set was preincubated without Hcy-thiolactone. Assays were carried out using black 96-well microtiter plates (OptiPlate-96F, Perkin Elmer). Pre-incubated tissue extracts (liver, 4 µL or heart, 40 µL) were diluted to 50 µL with assay buffer and mixed with 50 µL of reaction buffer prepared according to manufacturer's instruction. Fluorescence was measured at Ex/Em=540/590 nm for 20 or 30 min using a Tecan Infinite M200Pro plate reader. The rate of fluorescence increase in samples pre-incubated with Hcy-thiolactone was subtracted from the rate of fluorescence increase in the absence of Hcy-thiolactone. LOX activity is expressed as fluorescence units/min/µg protein.

Real-time PCR

Total RNA was extracted using Total RNA Purification Kit (Novazym), treated with DNase I (Thermo Scientific), and retrotranscribed using RiverAid Reverse Transcriptase (Thermo Scientific). Quantitative real-time PCR reactions were carried out using Eppendorf Mastercycler® ep realplex and iTaq Universal SYBR Green Supermix (Bio-Rad) following suppliers' protocols. The custom-designed primers (from Sigma Aldrich) were as follows:
Mouse Lox: forward 5'-TGCCAGTGGATTGATATTACAGATGT-3', reverse 5'-AGCGAATGTCACAGCGTACAA-3' (product length 124 bp);
Mouse Gapdh: forward 5'-CGTCCCGTAGACAAAATGGT-3', reverse 5'-TTGATGGCAACAATCTCCAC-3' (product length 110 bp);
Mouse β-actin: forward 5'-TGTTACCAACTGGGACGACA-3', reverse 5'- GGGGTGTTGAAGGTCTCAAA-3'.
Each reaction was carried out in duplicate for at least three individual mice of each *Cbs* genotype. The Pfaffl method (32) was used to calculate the relative Lox mRNA level normalized to Gapdh or β-actin mRNA level.

Statistics

Data are expressed as means±SD. For non-normally distributed variables, data were log-transformed. Comparisons between genotype groups were analyzed using a two-sided Student's *t*-test.

RESULTS

Cbs deficiency elevates plasma and urinary Hcy-thiolactone and *N*-Hcy-protein in mice

CBS-deficient patients are known to exhibit homocystinuria and HHcy. Similar to CBS-deficient humans, homozygous Cbs-deficient mice exhibit the HHcy phenotype (11, 33) and as shown here, a homocystinuria phenotype. We found that urinary tHcy levels were 68-fold elevated in $Cbs^{-/-}$ mice

compared to *Cbs*$^{+/-}$ littermates (from 68.7±4.7 to 4628±1105 μM, **Table I**); plasma tHcy was severely elevated (54-fold; from 5.0±2.6 to 272 ±50 μM), as previously described (11, 34). Urinary Hcy-thiolactone levels were elevated 100-fold (from <0.2 to 15.1±4.7 μM) in *Cbs*$^{-/-}$ mice relative to *Cbs*$^{+/-}$ animals. These Hcy-thiolactone values are the highest recorded in a mammalian organism (17, 35). Plasma *N*-Hcy-protein was elevated 11-fold, as previously described (34). Urinary *N*-Hcy-protein was 30-fold higher in *Cbs*$^{-/-}$ mice than in *Cbs*$^{+/-}$ animals.

_S_- and _N_-homocysteinylation status of mouse collagen

We asked whether collagen is targeted for *N*-homocysteinylation and whether such collagen modification might be affected by inactivation of the *Cbs* gene. To answer these questions we set out to detect and quantify *N*-Hcy in collagen from *Cbs*$^{-/-}$ mice and their *Cbs*$^{+/-}$ littermates.

We found that *N*-Hcy was present in total bone collagen preparations from *Cbs*$^{+/-}$ mice at 3.3 pmol *N*-Hcy/μg bone collagen. In *Cbs*$^{-/-}$ mouse, *N*-Hcy increased 14.6-fold to 49 pmol *N*-Hcy/μg bone collagen (**Fig. 1A**). We also found that acid-soluble tail collagen from *Cbs*$^{+/-}$ mice contained 0.7 pmol *N*-Hcy/μg collagen, which increased to 58 pmol *N*-Hcy/μg collagen in *Cbs*$^{-/-}$ animals (**Fig. 1B**).

Because Hcy is known to also bind to protein cysteine residues *via* disulfide bonds, we addressed a question of whether a disulfide-bound Hcy occurs in collagen. However, because mature collagen type I does not contain cysteine residues, we predicted that the only thiol groups that might be present in collagen molecules and engage in disulfide bond formation with free Hcy would come from the *N*-Hcy residues. To test this prediction we quantified *S*-Hcy in bone and tail collagen.

We found that *S*-Hcy levels in bone, tail, and heart collagen were equal to, or lower than, the corresponding *N*-Hcy levels. For example, in total bone collagen of *Cbs*$^{+/-}$ mice, *S*-Hcy was lower than *N*-Hcy (1.0 *vs*. 3.3 pmol *N*-Hcy/μg bone collagen, *P*=0.036; **Fig 1A**), while acetic acid-soluble tail collagen contained similar levels of *S*- and *N*-Hcy (1.3 *vs*. 0.7 pmol/μg tail collagen, *P*=0.43; **Fig. 1B**). In total heart collagen of *Cbs*$^{+/-}$ mice, *S*-Hcy was lower than *N*-Hcy (0.18 *vs*. 1.5 pmol *N*-Hcy/μg heart collagen, *P*=0.002; **Fig 1C**).

In *Cbs*$^{-/-}$ mice, both *S*- and *N*-Hcy were elevated; however, the *S*- and *N*-Hcy values were not significantly different from each other in the total bone collagen (30 *vs*. 49 pmol *N*-Hcy/μg bone collagen, *P*=0.31; **Fig 1A**) and acetic acid-soluble tail collagen (15.7 *vs*. 59 pmol *N*-Hcy/μg tail collagen, *P*=0.31; **Fig 1B**), while in total heart collagen, *S*-Hcy tended to be lower than *N*-Hcy (4.4 *vs*. 20.5 pmol *N*-Hcy/μg heart collagen, *P*=0.07; **Fig 1C**).

Identification of collagen lysine residues susceptible to _N_-homocysteinylation _in vitro_ and _in vivo_

To demonstrate that collagen is susceptible to *N*-homocysteinylation, we modified rat tail collagen type I with 50-fold molar excess of Hcy-thiolactone *in vitro*. Modified collagen was reduced,

derivatized, digested with trypsin, and subjected to LC-MS/MS analyses. Using the IAA-derivatization procedure, we identified seven *N*-Hcy-peptides (**Table II**), five in collagen type I alpha 1 chain (Col1A1) two in alpha 2 chain (Col1A2). Sequence coverage was 12% and 13% for Col1A1 and Col1A2, respectively. The *N*-Hcy-Lys residues were located at positions K160, K266, K583, K1085, K1225 in Col1A1 and positions K1070, K1146 in Col1A2. Residues K160 and K266 were also found to be *N*-homocysteinylated using the MMTS procedure (**Table II**). Two *N*-Hcy-Lys residues are located in the *N*-terminal (K^{266}) and *C*-terminal (K^{1085}) helical regions, one in the middle (K^{583}), and one (K^{160}) is located in the non-helical telopeptide region (**Fig. 2**) (36).

We also analyzed by LC-MS/MS tryptic peptides from collagen type I isolated from bones of *Cbs*$^{-/-}$ mice using the MMTS procedure. We identified one *N*-Hcy-peptide in Col1A1 containing *N*-Hcy-Lys residue at position K160 (**Table III**). Sequence coverage was 14-24%. Treatment of mouse bone collagen with Hcy-thiolactone led to *N*-homocystienylation of two additional residues: K266 in and K1070 in Col1A2 (**Table III**, **Fig. 2**). These results suggest that K160 is a predominant site of collagen *N*-homocysteinylation *in vivo*. Interestingly, the K160 residue in mouse Col1A1 corresponds to K170 in human Col1A1 that is known to be involved in pyridinoline crosslink formation (13).

Cbs gene inactivation affects collagen levels

In assessing effects of the *Cbs* gene inactivation on collagen crosslinking it is important to consider a possibility of changes in collagen levels in *Cbs*$^{-/-}$ mice relative to *Cbs*$^{+/-}$ animals. Thus, we quantified collagen levels in mouse tissues by hydroxyproline (Hyp) measurements in hydrolysates of collagen preparations from *Cbs*$^{-/-}$ mice and their *Cbs*$^{+/-}$ littermates. We found that collagen levels were significantly elevated in the heart (0.33 *vs*. 0.15 μg Hyp/mg heart, *P*=0.0003) (**Fig. 3A**) and tail (13.6 *vs*. 9.3 μg Hyp/mg dry tail, *P*=0.0003) (**Fig. 3B**) of *Cbs*$^{-/-}$ mice relative to *Cbs*$^{+/-}$ animals. In bone, collagen levels tended to be elevated in *Cbs*$^{-/-}$ relative to *Cbs*$^{+/-}$ mice (0.90 *vs*. 0.65 μg Hyp/mg bone, *P*=0.14) (**Fig. 3A**).

Cbs gene inactivation reduces collagen crosslinking

In order to examine whether HHcy affects collagen crosslinking we used a UPLC-based assay to quantify Pyd/Dpd levels in collagen isolated from tissues of *Cbs*$^{-/-}$ mice and their *Cbs*$^{+/-}$ littermates. To account for effects of HHcy on collagen levels we normalized Pyd/Dpd to collagen levels. We found that [Pyd/Dpd]/collagen ratios were reduced in the heart (426 *vs*. 717 pmol [Pyd/Dpd]/mg collagen, *P*=0.030) and tail collagen (61 *vs*. 291 pmol [Pyd/Dpd]/mg collagen, P<0.0001) and tended to be reduced in bone collagen (321 *vs*. 515 pmol [Pyd/Dpd] /mg collagen, *P*=0.059) in *Cbs*$^{-/-}$ mice relative to *Cbs*$^{+/-}$ animals (**Fig. 4**).

Collagen turnover

Connective tissue defects observed in HHcy could also be due to deranged collagen turnover. Tissue collagen turnover generates free and peptide-bound Dpd, which are released into the blood. To determine effects of HHcy due to Cbs deficiency on collagen degradation we quantified total Dpd using a competitive enzyme-linked immunoassay. Prior to the assay samples were acid-hydrolyzed to liberate Dpd from collagen peptides. We found that plasma Dpd levels were significantly reduced in *Cbs*$^{-/-}$ mice relative to their *Cbs*$^{+/-}$ littermates (0.92 *vs*. 2.74 nM, *P*=0.0003) (**Fig. 5**).

To further examine how Cbs deficiency affects collagen synthesis and degradation, we quantified plasma procollagen I C-terminal propeptide (PICP) and carboxyterminal telopeptide of collagen type I (CTX I) in *Cbs*$^{-/-}$ mice and their wild type littermates using a competitive enzyme-linked immunoassays. PICP, a marker of collagen synthesis, is cleaved off from procollagen during collagen biogenesis. CTX I, a marker of collagen turnover, contains sites of Dpd crosslinking and is cleaved off during type I collagen degradation in tissues; its serum levels are highly correlated to collagen turnover rate. As shown in **Table IV**, plasma CTX I levels were significantly lower in *Cbs*$^{-/-}$ mice relative to their *Cbs*$^{+/-}$ littermates (22.0 *vs*. 60.1 pg/mL, *P*=0.043). We also found that plasma PICP levels were not reduced, but tended to be increased in *Cbs*$^{-/-}$ mice relative to *Cbs*$^{+/-}$ animals (5.1±1.0 *vs*. 3.8±1.1 pg/mL, *P*=0.18) (**Table IV**), consistent with tissue collagen quantification by Hyp measurements (**Fig. 3**).

LOX activity and mRNA are not reduced by the *Cbs* gene inactivation

LOX [EC 1.4.3.13] is a copper-dependent oxidoreductase that catalyzes oxidative deamination of Lys residues to produce allysyl residues, ammonia and hydrogen peroxide. The generation of allysyl resides is required for subsequent formation of cross-links which stabilize collagen fibrils. Thus, it is possible that reduced levels of collagen crosslinking could be due to reduced LOX activity in *Cbs*$^{-/-}$ mice. To examine this possibility we quantified LOX activity in *Cbs*$^{-/-}$ mice and their *Cbs*$^{+/-}$ littermates. We found that LOX activity in the heart was similar in *Cbs*$^{-/-}$ and *Cbs*$^{+/-}$ mice: 9.4 *vs.* 10.1 units/min/μg protein, *P*=0.61 (**Table V**). Comparison of the assays in the presence and absence of the LOX inhibitor (Hcy-thiolactone), shows that most of the fluorescence signal (>90%) was associated with LOX. We also found that LOX activity in the liver was not affected by the *Cbs* genotype (3.5±1.8 *vs*. 2.4±0.4 units/min/μg protein, *P*=0.14).

We also quantified Lox mRNA by RT-qPCR. We found that Lox mRNA expression in the heart of *Cbs*$^{-/-}$ mice was elevated 1.88±0.18-fold relative to and *Cbs*$^{+/-}$ animals using Gapdh mRNA as a reference (**Fig. 6**). To confirm this finding, we additionally quantified Lox mRNA using β-actin as a reference and found that the results were similar: Lox mRNA was elevated 2.36±0.16-fold in *Cbs*$^{-/-}$ mice relative to *Cbs*$^{+/-}$ animals (**Fig. 6**). Taken together, these findings strongly suggest that neither Lox expression nor activity contribute to reduced levels of collagen crosslinks in *Cbs*$^{-/-}$ mice.

DISCUSSION

Since the discovery of clinical cases of severe HHcy in the 1960s, *CBS* deficiency has been known to cause connective tissue abnormalities (1). However, the underlying mechanism of these abnormalities was unknown. Since lysine residues are involved in intermolecular collagen crosslinking, we predicted that modification of collagen lysines by Hcy-thiolactone would impair crosslinking.

We used a *Cbs*$^{-/-}$ mouse model that recapitulates connective tissue abnormalities observed in CBS-deficient patients (11). We found that: 1) mouse bone, tail, and heart collagen is *N*-homocysteinylated *in vitro* and *in vivo*; 2) *N*-Hcy is elevated in *Cbs*$^{-/-}$ mouse collagen; 3) Pyd/Dpd crosslink levels are reduced in heart, bone, and tail collagen of *Cbs*$^{-/-}$ mice; 4) plasma soluble Dpd crosslink and crosslinked telopeptide CTX I are significantly reduced in *Cbs*$^{-/-}$ mice. 5) That these findings reflect a causal relationship between *N*-homocysteinylation and crosslinking, is supported by our LC-MS/MS experiments showing that *N*-homocysteinylation occurs at lysine residue K160, which is located in *N*-telopeptide of collagen type I alpha-1 chain, and which is involved in pyridinoline crosslink formation in *Cbs*$^{-/-}$ mice. 6) We also demonstrated that the reduction in pyridinoline crosslink level is not caused by lysine oxidase, whose expression and activity were not reduced by the *Cbs*$^{-/-}$ genotype. Taken together, our findings indicate that *N*-homocysteinylation impairs collagen crosslinking and thus provide a mechanistic explanation for connective tissue abnormalities observed in severe HHcy.

Collagen fibril assembly involves oxidation of lysine residues catalyzed by the Lox enzyme, which converts an εNH_2- group of a lysine residue to an aldehyde group, generating an allysine residue (**Fig. 6**). Allysine residues undergo spontaneous condensation with other lysine resides, generating Pyd and Dpd crosslinks in mature collagen fibers (**Fig. 6**). These intermolecular crosslinks are essential for mechanical properties and stability of collagen fibrils. Deficiencies in collagen crosslinking lead to connective tissue abnormalities (14, 15, 37). Our present findings strongly suggest that connective tissue abnormalities observed in HHcy are caused by *N*-homocysteinylation of lysine residue K160 located in the non-helical *N*-telopeptide region of Col1A1, which reduces the pyridinoline crosslink formation.

That HHcy may interfere with the collagen crosslink formation has been proposed in 1960s (38) and subsequently substantiated by studies that demonstrated reduced collagen crosslinking in CBS-deficient patients (39) and animal models of HHcy (40, 41). However, an underlying mechanism by which HHcy reduces collagen crosslinking remained unknown.

In the past, several attempts have been made to explain mechanistic basis of collagen crosslinking abnormalities in HHcy. For example, it has been suggested that defects in dermal

collagen in CBS-deficient patients are due to the condensation of Hcy with the precursor aldehyde residues (allysine) in collagen forming tetrahydrothiazine adducts (39). However, although free Hcy and aldehydes easily form stable tetrahydrothiazines (25, 42), such adducts have not been identified in collagen (39).

Biochemical studies of the Lox enzyme show that Hcy-thiolactone, a metabolite that accumulates in HHcy in mice and humans (34, 43), irreversibly inhibits the Lox enzyme activity by reacting with the active site lysine tyrosylquinone cofactor (31). However, our present findings that the Lox activity is not reduced by overproduction of Hcy-thiolactone in the *Cbs*$^{-/-}$ mouse model indicates that this reaction does not occur in this animal model.

Tissue culture studies suggest that reduced collagen crosslinking may be due to the inhibition of Lox enzymatic activity (31) and expression (44) by Hcy. For example, studies with cultured porcine vascular endothelial cells show that supplementation with Hcy inhibits Lox activity and down-regulates its expression; cysteine has a similar inhibitory effect on Lox activity (45). In cultured osteoblasts supplementation with Hcy inhibits the expression of Lox (44). However, it is not known whether these Lox-mediated mechanisms affect collagen crosslinking *in vivo* in HHcy patients or animal models. Our present findings clearly show that effects of HHcy on collagen crosslinking in *Cbs*$^{-/-}$ mice *are not* mediated by Lox.

Our previous studies have established that *N*-Hcy-protein is a significant component of Hcy metabolism in mice (34) and humans (19, 35) and identified over two dozen specific proteins (19, 22, 35) that carry *N*-Hcy, including human serum albumin (46-48) and fibrinogen (35, 49) which are *N*-homocysteinylated *in vivo* and in which specific *N*-Hcy-Lys residues have been identified. Our present findings, showing that K160 in mouse Col1A1 is *N*-homocysteinylated *in vivo*, add collagen to this list.

A preponderance of evidence strongly suggests that modification of protein lysine residues by Hcy-thiolactone, *i.e.* protein *N*-homocysteinylation, is involved in the pathology of HHcy (6). For example, *N*-Hcy-protein accumulates in plasma of CBS- or MTHFR-deficient patients who suffer from neurological and cardiovascular diseases (35). A clinical study found that plasma *N*-Hcy-protein is associated with coronary heart disease (50). In cardiac surgery patients, *N*-Hcy-protein accumulates in myocardium and aortas (51). Animal studies show that *N*-Hcy-protein accumulates within atherosclerotic lessions in aortas of *ApoE*$^{-/-}$ mice fed a normal chow diet, and increases in the animals fed a high-methionine diet that induces HHcy (51). Mechanistic studies suggest that *N*-homocysteinylation can cause disease by inducing amyloid-like structural transformation and generating toxic (52), pro-thrombotic (53), and autoimmunogenic proteins (42, 54).

Our present findings identify a novel pathogenic consequence of *N*-homocysteinylation—reduced pyridinoline crosslink formation in collagen—which provides a long-sought mechanistic explanation regarding how HHcy can lead to connective tissue abnormalities (38). These findings

support the following mechanism (**Fig. 7**). HHcy greatly enhances ATP-dependent metabolic conversion of Hcy to Hcy-thiolactone catalyzed by MetRS (**Table I** and ref (43)), illustrated by **Reactions 1a,b**.

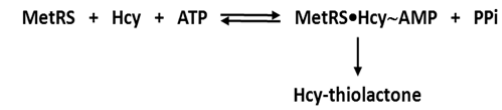

(**Reaction 1a**)

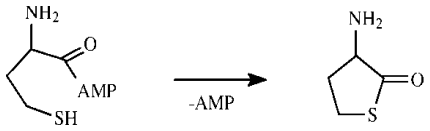

(**Reaction 1b**)

Hcy-thiolactone modifies lysine residues in collagen, which generates *N*-Hcy-collagen containing a free thiol group (**Reaction 2**).

εNH$_2$-Lys-collagen + Hcy-thiolactone → εNH-(Hcy-SH)-Lys-collagen (**Reaction 2**)

Because collagen type I, the most abundant of all collagens, does not contain cysteine residues in its primary structure, the -SH of *N*-Hcy residue is the sole thiol that is present in mature collagen trimers (**Fig. 7**). This thiol engages in a disulfide bond formation with a thiol of free Hcy affording *S*-Hcy (**Reaction 3**).

εNH-(Hcy-SH)-Lys-collagen + Hcy-SH → εNH-(Hcy-S-S-Hcy)-Lys-collagen (**Reaction 3**)

Concomitant with elevated levels of *N*-Hcy in collagen, we observed reductions in collagen Pyd/Dpd crosslinks levels in the bone, tail, heart (**Fig. 3**), and plasma (**Fig. 4**, **Table IV**) of *Cbs*$^{-/-}$ mice. These reductions in collagen crosslinking in *Cbs*$^{-/-}$ mice are consistent with the fact that crosslinking and *N*-homocysteinylation (**Table III**) both target the same lysine residue K160 located in the non-helical *N*-telopeptide region of Col1A1 (13, 36).

Our present *in vivo* findings that *N*-homocysteinylation impairs collagen crosslinking are consistent with an early *in vitro* study that examined relationships between chemical modifications of collagen lysine residues and crosslinking (55). That study found that modification of collagen lysine ε-amino groups with ethyl acetimidate prevented crosslinking, which was assessed indirectly by measuring collagen physicochemical properties such as molecular size and solubility (55).

Our findings that plasma levels of collagen degradation products, soluble Dpd crosslink and crosslinked C-terminal telopeptide of collagen type I (CTX I), were reduced in plasma of *Cbs*$^{-/-}$ mice suggest two scenarios: (i) reduced collagen crosslinking or (ii) suppressed bone collagen turnover in *Cbs*$^{-/-}$ mice relative to wild type animals. We favor the first scenario because mouse Cbs deficiency does not affect bone collagen level (**Fig. 3**), and tends to reduce crosslinking of bone collagen (**Fig. 4**). The second scenario is unlikely because plasma levels of PICP, a marker of collagen synthesis, were

not affected by *Cbs* genotype (**Table IV**). Thus, reduced levels of plasma total Dpd and CTX I reflect reduced crosslinking of bone collagen, most likely due to elevated *N*-homocysteinylation of collagen in *Cbs*$^{-/-}$ mice (**Fig. 1**). Plasma CTX I, but not markers of collagen I and III synthesis (PICP and *N*-terminal propeptide of procollagen III), are reduced also in CBS-deficient patients (56), which suggests that HHcy similarly effects collagen metabolism in mice and humans.

Lox is responsible for the first step in crosslink formation by oxidizing collagen lysine residues to allysine. Because decreased level of Lox activity impairs crosslinking (15), it was possible that reduced collagen pyridinoline crosslinks in *Cbs*$^{-/-}$ mice could be caused by reduced Lox expression and/or activity. However, our results exclude this possibility by showing that Lox expression and activity were not reduced by the *Cbs*$^{-/-}$ genotype (**Table V**, **Fig. 6**).

Our findings that collagen levels were elevated in the tail and heart of *Cbs*$^{-/-}$ mice suggest that dysregulated collagen accumulation can also contribute to connective tissue deficiencies in severe HHcy. That HHcy can enhance collagen synthesis and accumulation has been demonstrated by previous findings in cultured smooth muscle (57) and liver (58) cells treated with Hcy and in livers of mice with HHcy induced by a high-Met diet (58).

In conclusion, our data support a mechanism that explains at least in part the connective tissue abnormalities observed in HHcy mice and humans. In this mechanism HHcy increases the conversion of Hcy to, and accumulation of, Hcy-thiolactone, which then causes *N*-homocysteinylation of collagen lysine residues, which in turn impairs the formation of pyridinoline crosslinks important for collagen fibril structure/function. Our data point to a critical role of lysine residue K160 located in *N*-telopeptide of Col1A1 in this mechanism. Tissue-specific alterations in collagen accumulation can also contribute to connective tissue abnormalities in HHcy.

Acknowledgements: We thank Warren Kruger for a breeding pair of *Tg-I278T Cbs*$^{+/-}$ mice.

Conflict of interest: The authors declare that they have no conflicts of interest with the contents of this article.

REFERENCES

1. Mudd, S. H., Levy, H. L., and Krauss, J. P. (2001) Disorders of transsulfuration. In *The metabolic and molecular bases of inherited disease* (Scriver, C. R., Beaudet, A. L., Sly, W. S., Valle, D., Childs, B., Kinzler, K. W., and Vogelstein, B., eds) Vol. 2 pp. 2007-2056, Mc Graw-Hill, New York
2. Jakubowski, H., and Goldman, E. (1993) Synthesis of homocysteine thiolactone by methionyl-tRNA synthetase in cultured mammalian cells. *FEBS letters* **317**, 237-240
3. Jakubowski, H. (1997) Metabolism of homocysteine thiolactone in human cell cultures. Possible mechanism for pathological consequences of elevated homocysteine levels. *The Journal of biological chemistry* **272**, 1935-1942

4. Jakubowski, H. (2000) Homocysteine thiolactone: metabolic origin and protein homocysteinylation in humans. *The Journal of nutrition* **130**, 377S-381S
5. Jakubowski, H., Zhang, L., Bardeguez, A., and Aviv, A. (2000) Homocysteine thiolactone and protein homocysteinylation in human endothelial cells: implications for atherosclerosis. *Circulation research* **87**, 45-51
6. Jakubowski, H. (2013) *Homocysteine in Protein Structure/Function and Human Disease - Chemical Biology of Homocysteine-containing Proteins*, Springer, Wien
7. Jakubowski, H., Borowczyk, K., Glowacki, R., and Nygård, O. (2015) Urinary Homocysteine Thiolactone Predicts Acute Myocardial Infarction in a Randomized Controlled Homocysteine-lowering B-vitamin Trial. *Circulation* **132**, A19250
8. McLean, R. R., Karasik, D., Selhub, J., Tucker, K. L., Ordovas, J. M., Russo, G. T., Cupples, L. A., Jacques, P. F., and Kiel, D. P. (2004) Association of a common polymorphism in the methylenetetrahydrofolate reductase (MTHFR) gene with bone phenotypes depends on plasma folate status. *J Bone Miner Res* **19**, 410-418
9. Abrahamsen, B., Jorgensen, H. L., Nielsen, T. L., Andersen, M., Haug, E., Schwarz, P., Hagen, C., and Brixen, K. (2006) MTHFR c.677C>T polymorphism as an independent predictor of peak bone mass in Danish men--results from the Odense Androgen Study. *Bone* **38**, 215-219
10. Robert, K., Maurin, N., Vayssettes, C., Siauve, N., and Janel, N. (2005) Cystathionine beta synthase deficiency affects mouse endochondral ossification. *Anat Rec A Discov Mol Cell Evol Biol* **282**, 1-7
11. Gupta, S., Kuhnisch, J., Mustafa, A., Lhotak, S., Schlachterman, A., Slifker, M. J., Klein-Szanto, A., High, K. A., Austin, R. C., and Kruger, W. D. (2009) Mouse models of cystathionine beta-synthase deficiency reveal significant threshold effects of hyperhomocysteinemia. *FASEB journal : official publication of the Federation of American Societies for Experimental Biology* **23**, 883-893
12. Gelse, K., Poschl, E., and Aigner, T. (2003) Collagens--structure, function, and biosynthesis. *Adv Drug Deliv Rev* **55**, 1531-1546
13. Eyre, D. R., Weis, M. A., and Wu, J. J. (2008) Advances in collagen cross-link analysis. *Methods* **45**, 65-74
14. Hornstra, I. K., Birge, S., Starcher, B., Bailey, A. J., Mecham, R. P., and Shapiro, S. D. (2003) Lysyl oxidase is required for vascular and diaphragmatic development in mice. *The Journal of biological chemistry* **278**, 14387-14393
15. Maki, J. M., Rasanen, J., Tikkanen, H., Sormunen, R., Makikallio, K., Kivirikko, K. I., and Soininen, R. (2002) Inactivation of the lysyl oxidase gene Lox leads to aortic aneurysms, cardiovascular dysfunction, and perinatal death in mice. *Circulation* **106**, 2503-2509
16. Fujimoto, D., Moriguchi, T., Ishida, T., and Hayashi, H. (1978) The structure of pyridinoline, a collagen crosslink. *Biochemical and biophysical research communications* **84**, 52-57
17. Jakubowski, H. (2013) *Homocysteine in protein structure/function and human disease*, Springer
18. Jakubowski, H. (2008) New method for the determination of protein N-linked homocysteine. *Analytical Biochemistry* **380**, 257-261
19. Jakubowski, H. (2002) Homocysteine is a protein amino acid in humans. Implications for homocysteine-linked disease. *The Journal of biological chemistry* **277**, 30425-30428
20. Jakubowski, H. (2002) The determination of homocysteine-thiolactone in biological samples. *Analytical biochemistry* **308**, 112-119
21. Chwatko, G., and Jakubowski, H. (2005) Urinary excretion of homocysteine-thiolactone in humans. *Clinical chemistry* **51**, 408-415
22. Jakubowski, H. (2008) New method for the determination of protein N-linked homocysteine. *Analytical biochemistry* **380**, 257-261
23. Bradford, M. M. (1976) A rapid and sensitive method for the quantitation of microgram quantities of protein utilizing the principle of protein-dye binding. *Anal Biochem* **72**, 248-254

24. Chwatko, G., and Jakubowski, H. (2005) The determination of homocysteine-thiolactone in human plasma. *Analytical biochemistry* **337**, 271-277
25. Jakubowski, H. (2006) Mechanism of the condensation of homocysteine thiolactone with aldehydes. *Chemistry* **12**, 8039-8043
26. Perła-Kaján, J., Gryszczyńska, A., Mielcarek, S., and Jakubowski, H. (2011) Cation exchange HPLC analysis of desmosines in elastin hydrolysates. *Anal Bioanal Chem* **401**, 2473-2479
27. Edwards, C. A., and O'Brien, W. D. (1980) Modified assay for determination of hydroxyproline in a tissue hydrolyzate. *Clin Chim Acta* **104**, 161-167
28. Jakubowski, H. (1999) Protein homocysteinylation: possible mechanism underlying pathological consequences of elevated homocysteine levels. *FASEB journal : official publication of the Federation of American Societies for Experimental Biology* **13**, 2277-2283
29. Telser, A., and Rovin, B. (1980) A specific stain for sulfhydryl groups in proteins after separation by polyacrylamide gel electrophoresis. *Biochimica et biophysica acta* **624**, 363-371
30. Bakun, M., Niemczyk, M., Domanski, D., Jazwiec, R., Perzanowska, A., Niemczyk, S., Kistowski, M., Fabijanska, A., Borowiec, A., Paczek, L., and Dadlez, M. (2012) Urine proteome of autosomal dominant polycystic kidney disease patients. *Clin Proteomics* **9**, 13
31. Liu, G., Nellaiappan, K., and Kagan, H. M. (1997) Irreversible inhibition of lysyl oxidase by homocysteine thiolactone and its selenium and oxygen analogues. Implications for homocystinuria. *The Journal of biological chemistry* **272**, 32370-32377
32. Pfaffl, M. W. (2001) A new mathematical model for relative quantification in real-time RT-PCR. *Nucleic acids research* **29**, e45
33. Watanabe, M., Osada, J., Aratani, Y., Kluckman, K., Reddick, R., Malinow, M. R., and Maeda, N. (1995) Mice deficient in cystathionine beta-synthase: animal models for mild and severe homocyst(e)inemia. *Proceedings of the National Academy of Sciences of the United States of America* **92**, 1585-1589
34. Jakubowski, H., Perla-Kajan, J., Finnell, R. H., Cabrera, R. M., Wang, H., Gupta, S., Kruger, W. D., Kraus, J. P., and Shih, D. M. (2009) Genetic or nutritional disorders in homocysteine or folate metabolism increase protein N-homocysteinylation in mice. *FASEB journal : official publication of the Federation of American Societies for Experimental Biology* **23**, 1721-1727
35. Jakubowski, H., Boers, G. H., and Strauss, K. A. (2008) Mutations in cystathionine beta-synthase or methylenetetrahydrofolate reductase gene increase N-homocysteinylated protein levels in humans. *FASEB journal : official publication of the Federation of American Societies for Experimental Biology* **22**, 4071-4076
36. Fledelius, C., Johnsen, A. H., Cloos, P. A., Bonde, M., and Qvist, P. (1997) Characterization of urinary degradation products derived from type I collagen. Identification of a beta-isomerized Asp-Gly sequence within the C-terminal telopeptide (alpha1) region. *The Journal of biological chemistry* **272**, 9755-9763
37. Takaluoma, K., Hyry, M., Lantto, J., Sormunen, R., Bank, R. A., Kivirikko, K. I., Myllyharju, J., and Soininen, R. (2007) Tissue-specific changes in the hydroxylysine content and cross-links of collagens and alterations in fibril morphology in lysyl hydroxylase 1 knock-out mice. *The Journal of biological chemistry* **282**, 6588-6596
38. McKusick, V. A. (1966) *Heritable Disorders of Connective Tissue, p. 155*, Mosby, C.V., St Louis
39. Kang, A. H., and Trelstad, R. L. (1973) A collagen defect in homocystinuria. *J Clin Invest* **52**, 2571-2578
40. Saito, M., Marumo, K., Soshi, S., Kida, Y., Ushiku, C., and Shinohara, A. (2010) Raloxifene ameliorates detrimental enzymatic and nonenzymatic collagen cross-links and bone strength in rabbits with hyperhomocysteinemia. *Osteoporos Int* **21**, 655-666
41. Griffiths, R., Tudball, N., and Thomas, J. (1976) Effect of induced elevated plasma levels of homocystine and methionine in rats on collagen and elastin structures. *Connect Tissue Res* **4**, 101-106

42. Undas, A., Perla, J., Lacinski, M., Trzeciak, W., Kazmierski, R., and Jakubowski, H. (2004) Autoantibodies against N-homocysteinylated proteins in humans: implications for atherosclerosis. *Stroke* **35**, 1299-1304
43. Chwatko, G., Boers, G. H., Strauss, K. A., Shih, D. M., and Jakubowski, H. (2007) Mutations in methylenetetrahydrofolate reductase or cystathionine beta-synthase gene, or a high-methionine diet, increase homocysteine thiolactone levels in humans and mice. *FASEB journal : official publication of the Federation of American Societies for Experimental Biology* **21**, 1707-1713
44. Thaler, R., Agsten, M., Spitzer, S., Paschalis, E. P., Karlic, H., Klaushofer, K., and Varga, F. (2011) Homocysteine suppresses the expression of the collagen cross-linker lysyl oxidase involving IL-6, Fli1, and epigenetic DNA methylation. *The Journal of biological chemistry* **286**, 5578-5588
45. Raposo, B., Rodriguez, C., Martinez-Gonzalez, J., and Badimon, L. (2004) High levels of homocysteine inhibit lysyl oxidase (LOX) and downregulate LOX expression in vascular endothelial cells. *Atherosclerosis* **177**, 1-8
46. Sikora, M., Marczak, L., Twardowski, T., Stobiecki, M., and Jakubowski, H. (2010) Direct monitoring of albumin lysine-525 N-homocysteinylation in human serum by liquid chromatography/mass spectrometry. *Analytical biochemistry* **405**, 132-134
47. Marczak, L., Sikora, M., Stobiecki, M., and Jakubowski, H. (2011) Analysis of site-specific N-homocysteinylation of human serum albumin in vitro and in vivo using MALDI-ToF and LC-MS/MS mass spectrometry. *Journal of proteomics* **74**, 967-974
48. Glowacki, R., and Jakubowski, H. (2004) Cross-talk between Cys34 and lysine residues in human serum albumin revealed by N-homocysteinylation. *The Journal of biological chemistry* **279**, 10864-10871
49. Sikora, M., Marczak, L., Kubalska, J., Graban, A., and Jakubowski, H. (2014) Identification of N-homocysteinylation sites in plasma proteins. *Amino acids* **46**, 235-244
50. Yang, X., Gao, Y., Zhou, J., Zhen, Y., Yang, Y., Wang, J., Song, L., Liu, Y., Xu, H., Chen, Z., and Hui, R. (2006) Plasma homocysteine thiolactone adducts associated with risk of coronary heart disease. *Clinica chimica acta; international journal of clinical chemistry* **364**, 230-234
51. Perla-Kajan, J., Stanger, O., Luczak, M., Ziolkowska, A., Malendowicz, L. K., Twardowski, T., Lhotak, S., Austin, R. C., and Jakubowski, H. (2008) Immunohistochemical detection of N-homocysteinylated proteins in humans and mice. *Biomedicine & pharmacotherapy = Biomedecine & pharmacotherapie* **62**, 473-479
52. Paoli, P., Sbrana, F., Tiribilli, B., Caselli, A., Pantera, B., Cirri, P., De Donatis, A., Formigli, L., Nosi, D., Manao, G., Camici, G., and Ramponi, G. (2010) Protein N-homocysteinylation induces the formation of toxic amyloid-like protofibrils. *Journal of molecular biology* **400**, 889-907
53. Sauls, D. L., Lockhart, E., Warren, M. E., Lenkowski, A., Wilhelm, S. E., and Hoffman, M. (2006) Modification of fibrinogen by homocysteine thiolactone increases resistance to fibrinolysis: a potential mechanism of the thrombotic tendency in hyperhomocysteinemia. *Biochemistry* **45**, 2480-2487
54. Undas, A., Jankowski, M., Twardowska, M., Padjas, A., Jakubowski, H., and Szczeklik, A. (2005) Antibodies to N-homocysteinylated albumin as a marker for early-onset coronary artery disease in men. *Thrombosis and haemostasis* **93**, 346-350
55. Tanzer, M. L. (1968) Intermolecular cross-links in reconstituted collagen fibrils. Evidence for the nature of the covalent bonds. *The Journal of biological chemistry* **243**, 4045-4054
56. Lubec, B., Fang-Kircher, S., Lubec, T., Blom, H. J., and Boers, G. H. (1996) Evidence for McKusick's hypothesis of deficient collagen cross-linking in patients with homocystinuria. *Biochimica et biophysica acta* **1315**, 159-162
57. Majors, A., Ehrhart, L. A., and Pezacka, E. H. (1997) Homocysteine as a risk factor for vascular disease. Enhanced collagen production and accumulation by smooth muscle cells. *Arteriosclerosis, thrombosis, and vascular biology* **17**, 2074-2081

58. Lei, W., Long, Y., Li, S., Liu, Z., Zhu, F., Hou, F. F., and Nie, J. (2015) Homocysteine Induces Collagen I Expression by Downregulating Histone Methyltransferase G9a. *PloS one* **10**, e0130421

FOOTNOTES

This study was supported in part by grants from the National Science Center, Poland (2011/02/A/NZ1/00010, 2012/07/B/NZ7/01178, 2013/09/B/NZ5/02794, 2013/11/B/NZ1/00091, 2014/15/B/NZ2/01079), and the American Heart Association (0855919D, 12GRNT9420014).

The abbreviations used are: bp, base pairs; Cbs, cystathionine β-synthase; Col1A1, collagen alpha-1(I) chain; CTX I, carboxyterminal telopeptide of collagen type I; Dpd, deoxypyridinoline; DTT, dithiothreitol; Hcy, homocysteine; HHcy, hyperhomocysteinemia; HPLC, high performance liquid chromatography; IAA, iodoacetamide; LC, liquid chromatography; Lox, lysyl oxidase; MetRS, methionyl-tRNA synthetase; MMTS, methyl methanethiosulfonate; MS, mass spectrometry; *N*-Hcy, Hcy linked to a protein *via* an isopeptide bond with ε-amino group of a lysine residue; PICP, procollagen I C-terminal propeptide; Pyd, pyridinoline; TCEP, tris(2-carboxyethyl) phosphine; tHcy, total Hcy; *S*-Hcy, Hcy linked to a protein *via* a disulfide bond with a protein thiol; *N*-Hcy, Hcy linked to a protein *via* an isopeptide bond with an ε-amino group of a lysine residue.

FIGURE LEGENDS

Figure 1. Collagen *N*- and *S*-Hcy are elevated in *Cbs*$^{-/-}$ mice. *N*-and *S*-Hcy were quantified by HPLC in total bone collagen (panel **A.**), acid-soluble tail collagen (panel **B.**), and total heart collagen from *Cbs*$^{-/-}$ and *Cbs*$^{+/-}$ mice. Asterisks (*) denote significant (P<0.05) differences between *Cbs*$^{-/-}$ (n=4-5) and *Cbs*$^{+/-}$ (n=4-6) mice. *P* values shown are for comparisons between *N*-and *S*-linked Hcy levels.

Figure 2. Localization of *N*-homocysteinylation and crosslinking sites in the primary structure of collagen type I alpha-1 chain. *N*-homocysteinylation sites were identified by LC-MS/MS in the present work. Crosslinking sites were identified by other investigators (13). The amino acid sequence of mature mouse Col1A1 (residues 152-1207 of procollagen) is from http://www.uniprot.org/uniprot/P11087. *N*- and *C*-terminal nonhelical telopeptide regions are underlined. Peptides containing *N*-Hcy are indicated in boldface. Lysine residue susceptible to *N*-homocysteinylation *in vitro* and *in vivo* (**K**^{160}) is indicated by a superscript number. Lysine residues susceptible to *N*-homocysteinylation only *in vitro* (***K***^{266}, ***K***^{584}, ***K***^{1085}) are indicated by superscript numbers and italicized. Lysine residues **K**^{160}, K^{254}, K^{1097}, K^{1197} corresponding to homologous lysines in human Col1A1 that are involved in pyridinoline crosslink formation, are highlighted in gray.

Figure 3. Collagen content in tissues of *Cbs*$^{-/-}$ and *Cbs*$^{+/-}$ mice. Collagen was quantified in the bone, heart (panel **A.**), and tail (panel **B.**) by measurements of hydroxyproline in tissue hydrolysates. The values shown for the heart and bone were obtained with 4-6 mice, while the values for the tail were obtained with 12-20 mice for each genotype.

Figure 4. Reduced collagen crosslinking in *Cbs*$^{-/-}$ mice. Pyd/Dpd crosslinks were quantified using an UPLC assay in heart (n=5-6), bone (n=5-6), and tail (n=16-23) collagen from *Cbs*$^{-/-}$ (n=6-16) and *Cbs*$^{+/-}$ (n=5-23) mice. *P* values shown are for comparisons between *Cbs*$^{-/-}$ and *Cbs*$^{+/-}$ mice. Asterisks (*) indicate significant (p<0.05) effect of the *Cbs* genotype.

Figure 5. Reduced plasma Dpd levels in *Cbs*$^{-/-}$ mice. Dpd was quantified by a competitive immunoassay in acid-hydrolyzed plasma samples from *Cbs*$^{-/-}$ (n=7) and *Cbs*$^{+/-}$ (n=10) mice.

Figure 6. Increased Lox mRNA expression in the hearts of *Cbs*$^{-/-}$ mice. Lox expression was quantified by real-time PCR. *p<0.05 for *Cbs*$^{-/-}$ (n=3) *vs*. *Cbs*$^{+/-}$ (n=3) mice.

Figure 7. Schematic representation of collagen *N*-homocysteinylation and pyridinoline crosslink formation. See text for discussion.

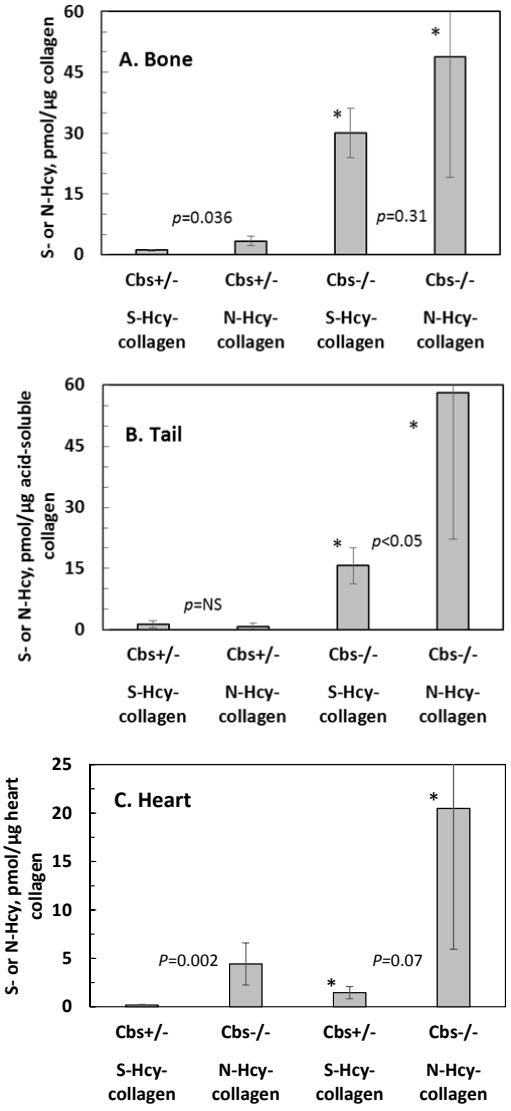
A. Bone
S- or N-Hcy, pmol/µg collagen
60
45
30
15
0
*
*
p=0.036
p=0.31
Cbs+/-
S-Hcy-collagen
Cbs+/-
N-Hcy-collagen
Cbs-/-
S-Hcy-collagen
Cbs-/-
N-Hcy-collagen
B. Tail
S- or N-Hcy, pmol/µg acid-soluble collagen
60
45
30
15
0
*
*
p<0.05
p=NS
Cbs+/-
S-Hcy-collagen
Cbs+/-
N-Hcy-collagen
Cbs-/-
S-Hcy-collagen
Cbs-/-
N-Hcy-collagen
C. Heart
S- or N-Hcy, pmol/µg heart collagen
25
20
15
10
5
0
*
*
P=0.002
P=0.07
Cbs+/-
S-Hcy-collagen
Cbs-/-
N-Hcy-collagen
Cbs+/-
S-Hcy-collagen
Cbs-/-
N-Hcy-collagen

Fig. 1

152QMSYGYDEK[160]SAGVSVPGPMGPSGPRGLPGPPGAPGPQGFQGPPGEPGEPGGSGPMGPRGPPGPPGKNGDDGEAGKPGRPGERGPPGPQGARGLPGTAGLPGMKGHR**GFSGLDGAK[266]GDAGPAGPK**
GEPGSPGENGAPGQMGPRGLPGERGRPGPPGTAGARGNDGAVGAAGPPGPTGPTGPPGFPGAVGAKGEAGPQGARGSEGPQGVRGEPGPPGPAGAAGPAGNPGADGQPGAKGANGAPGIAGAPGFPGARGPSG
PQGPSGPPGPKGNSGEPGAPGNKGDTGAKGEPGATGVQGPPGPAGEEGKRGARGEPGPSGLPGPPGERGGPGSRGFPGADGVAGPKGPSGERGAPGPAGPKGSPGEAGRPGEAGLPGAKGLTGSPGSPGPDGKTGP
PGPAGQDGRPGPAGPPGARGQAGVMGFPGPK**GTAGEPGK[583]AGER**GLPGPPGAVGPAGKDGEAGAQGAPGPAGPAGERGEQGPAGSPGFQGLPGPAGPPGEAGKPGEQGVPGDLGAPGPSGARGERGFPGERG
VQGPPGPAGPRGNNGAPGNDGAKGDTGAPGAPGSQGAPGLQGMPGERGAAGLPGPKGDRGDAGPKGADGSPGKDGARGLTGPIGPPGPAGAPGDKGEAGPSGPPGPTGARGAPGDRGEAGPPGPAGFAGPPGA
DGQPGAKGEPGDTGVKGDAGPPGPAGPAGPPGPIGNVGAPGPKGPRGAAGPPGATGFPGAAGRVGPPGPSGNAGPPGPPGPVGKEGGKGPRGETGPAGRPGEVGPPGPPGPAGEKGSPGADGPAGSPGTPGPQGI
AGQRGVVGLPGQRGERGFPGLPGPSGEPGKQGPSGSSGERGPPGPMGPPGLAGPPGESGREGSPGAEGSPGRDGAPGAKGDRGETGPAGPPGAPGAPGAPGPVGPAGKNGDRGETGPAGPAGPIGPAGARGPAGP
QGPR**GDK[1085]GETGEQGD**RGIKGHRGFSGLQGPPGSPGSPGEQGPSGASGPAGPRGPPGSAGSPGKDGLNGLPGPIGPPGPRGRTGDSGPAGPPGPPGPPGPPGPPSGGYDFSFLPQPPQEKSQDGGRYYRA**1207**

Fig. 2

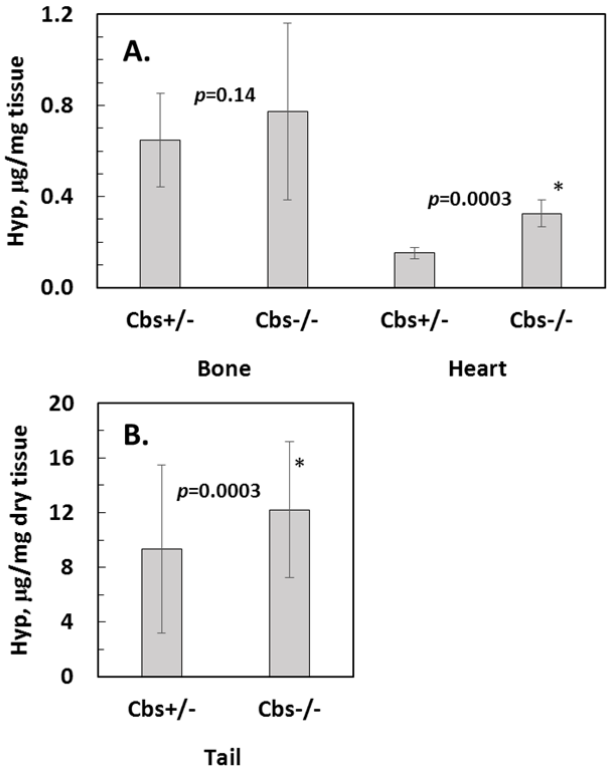

Fig. 3

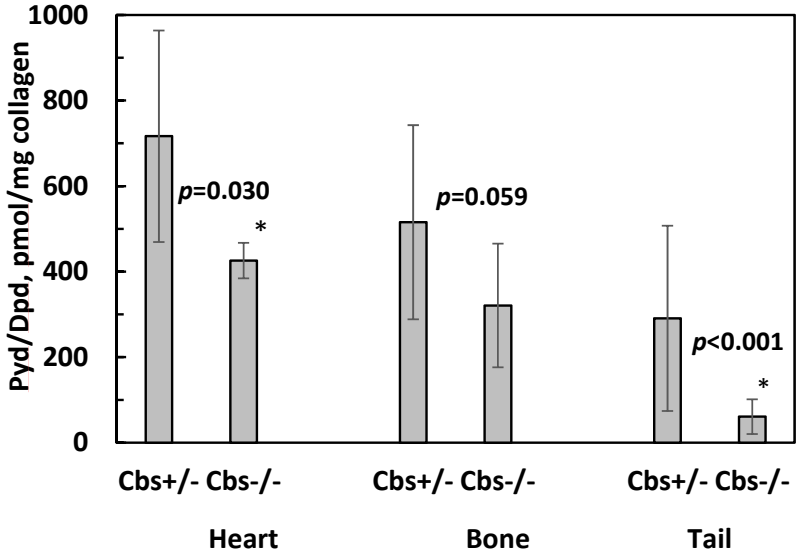
1000
800
600
400
200
0
Pyd/Dpd, pmol/mg collagen
p=0.030
*
p=0.059
p<0.001
*
Cbs+/-
Cbs-/-
Cbs+/-
Cbs-/-
Cbs+/-
Cbs-/-
Heart
Bone
Tail

Fig. 4

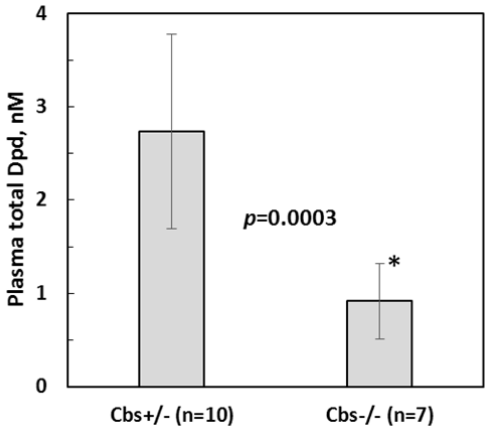
Plasma total Dpd, nM
4
3
2
1
0
p=0.0003
*
Cbs+/- (n=10)
Cbs-/- (n=7)

Fig. 5

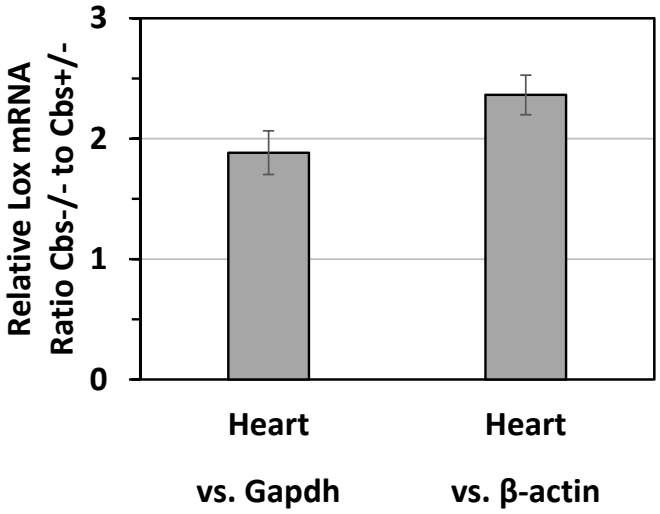
Relative Lox mRNA
Ratio Cbs-/- to Cbs+/-
3
2
1
0
Heart
vs. Gapdh
Heart
vs. β-actin

Fig. 6

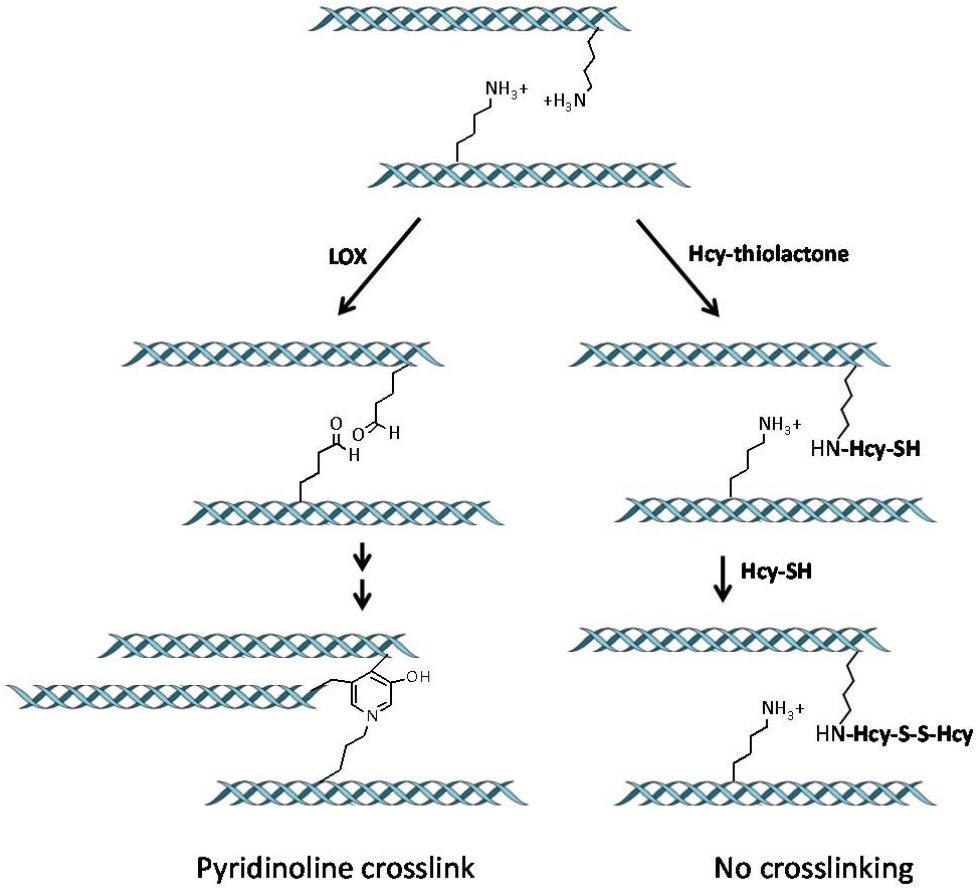
LOX
Hcy-thiolactone
HN-Hcy-SH
Hcy-SH
HN-Hcy-S-S-Hcy
Pyridinoline crosslink
No crosslinking

Fig. 7

TABLE I. *Plasma and urinary N-Hcy-protein, Hcy-thiolactone, and tHcy are severely elevated in Cbs-deficient mice* [a]

Genotype (n)	*N*-Hcy-protein, µM	Hcy-thiolactone, µM	tHcy, µM
Plasma			
Cbs$^{-/-}$ (4)	16.6±4.1		272±50
Cbs$^{+/-}$ (4)	1.5±0.2	0.006±0.0002	5.0±2.6
Urine			
Cbs$^{-/-}$ (6)	15.1±4.7	11.8±0.9	4628±1105
Cbs$^{+/-}$ (6)	0.5±0.2	<0.2	69 ±16

[a] Data are shown as means±SD.

TABLE II. *N-Hcy-peptides identified by LC-MS/MS in rat tail collagen type I modified with Hcy-thiolactone in vitro* [a]

Collagen type I *N*-Hcy-peptide	Chain	Ion score	*N*-Hcy-Lys residue no.	Start-end
Procedure with DTT reduction and IAA modification				
QMSYGYDE**K**^{Hcy}SAGVSVPGPMGPSGPR	Alpha 1	88	160	152–176
GFSGLDGA**K**^{Hcy}GDTGPAGPK	Alpha 1	139	266	258-275
GTAGEPG**K**^{Hcy}AGER	Alpha 1	59	583	576-587
GD**K**^{Hcy}GETGEQGDR	Alpha 1	72	1085	1083-1094
DLEVDTTL**K**^{Hcy}SLSQQIENIR	Alpha 1	146	1225	1217-1235
GPAGPSGPIG**K**^{Hcy}DGR	Alpha 2	133	1070	1060-1073
DYEVDATL**K**^{Hcy}SLNNQIETLLTPEGSR	Alpha 2	67	1128	1120-1144
Procedure with TCEP reduction and MMTS thiolation				
GPPGPLGLGGNFASQMSYGYDE**K**^{Hcy}SAGVSVPGPM GPSGPR	Alpha 1	76	160[b]	138-176
PGPPGPPGPPGPPGLGGNFASQMSYGYDE**K**^{Hcy}SAGV SVPGPMGPSGPR	Alpha 1	89	160[c]	131-176
GFSGLDGA**K**^{Hcy}GDTGPAGPK	Alpha 1	123	266[c]	258-275

K^{Hcy} denotes *N*-Hcy-Lys residue.
[a] Collagen peptides were analyzed using the IAA or MMTS sample preparation procedure.
[b] Identified in native collagen
[c] Identified in native collagen treated with Hcy-thiolactone

TABLE III. *N-Hcy-peptides identified by LC-MS/MS in Cbs$^{-/-}$ mouse bone collagen type I* [a]

Collagen type I *N*-Hcy-peptide	Chain	Ion score	*N*-Hcy-Lys residue no.	Start-end
PGLGGNFASQMSYGYDE**K**^{Hcy}SAGVSVPGPMGPSGPR	Alpha 1	64	160[b]	143-176
DE**K**^{Hcy}SAGVSVPGPMGPSGPR	Alpha 1	77	160[c]	158-176
GFSGLDGA**K**^{Hcy}GDTGPAGPK	Alpha 1	91	266[c]	258-275
GPAGPSGPIG**K**^{Hcy}DGR	Alpha 2	110	1070[c]	1060-1073

K^{Hcy} denotes *N*-Hcy-Lys residue
[a] Collagen was reduced with TCEP and thiolated with MMTS
[b] Identified in native collagen
[c] Identified in native collagen treated with Hcy-thiolactone

TABLE IV. *Levels of plasma carboxyterminal telopeptide of collagen type I (CTX I) and procollagen I C-terminal propeptide (PICP) in Cbs$^{-/-}$ and Cbs$^{+/-}$ mice* [a]

Genotype (n)	Age, days	Plasma tHcy, µM	Plasma CTXI			Plasma PICP, pg/mL
			Median (range), pg/mL	Log transformed adjusted mean, ln[pg/mL]	Adjusted original scale, (pg/mL)	
Cbs$^{+/-}$(n=20)	293±50	10.5±4.5	68.6 (2-342)	4.1±1.4	60.1	3.8±1.1
Cbs$^{-/-}$(n=26)	285±50	251±53	37.6 (1-292)	3.1±1.7	22.0	5.1±1.0
P value		<0.001			0.043	0.18

[a] Data are shown as means±SD. P values were calculated using two-tailed *t*-test. Adjusted means for plasma CTXI were calculated using the log-transformed data. These were exponentiated to obtain adjusted values on the original scale.

TABLE V. *LOX activity in Cbs$^{-/-}$ and Cbs$^{+/-}$ mice* [a]

Genotype	Heart	Liver
	LOX activity inhibited by Hcy-thiolactone, Fluorescence units/min/µg protein	
Cbs$^{-/-}$	9.4±2.4 (n=4)	3.5±1.8 (n=10)
Cbs$^{+/-}$	10.1±1.0 (n=4)	2.4±0.4 (n=6)
	Total activity, Fluorescence units/min/µg protein	
Cbs$^{-/-}$	10.3±8.4 (n=15)	23.1±8.5 (n=15)
Cbs$^{+/-}$	8.4±3.8 (n=15)	20.0±6.8 (n=14)
Differences between genotypes are not statistically significant, *P* values=0.14 to 0.61		